Controlled Molecular Architectures in Microfluidic Immunosensors for Detecting *Staphylococcus aureus*

Andrey Coatrini Soares[1*], Juliana Coatrini Soares[1], Valquiria Cruz Rodrigues[2], Osvaldo N. Oliveira Jr[2], Luiz Henrique Capparelli Mattoso[1]

[1] Nanotechnology National Laboratory for Agriculture (LNNA), Embrapa Instrumentação, 13560-970 São Carlos, SP, Brazil.

[2]São Carlos Institute of Physics, University of São Paulo,13566-590 São Carlos, Brazil

*Corresponding Author: andreycoatrini@gmail.com

Section 1: Obtaining capacitance from impedance

Impedance spectra are measured by applying an alternating voltage with a given amplitude, phase and frequency, generating alternating current. Both are expressed according to equation S1 and S2.

$$V(t) = V_0 e^{j\omega t} \qquad \text{(S1)}$$

$$I(t) = I_0 e^{j(\omega t - \phi)} \qquad \text{(S2)}$$

Complex impedance is calculated with the relationship (eq. S3) between voltage V (t) and current I (t), where Z' is the real impedance, Z” is the imaginary impedance, $j = \sqrt{-1}$ and ϕ is the phase.

$$Z^* = \frac{V(t)}{I(t)} = \frac{V_0 e^{j\omega t}}{I_0 e^{j(\omega t - \phi)}} \left| Z^* \right| e^{j\phi} = Z' + jZ'' \qquad \text{(S3)}$$

Biosensors built in this microfluidic chips have a capacitive character, and therefore we shall use the concept of complex capacitance defined in eq. S4, in which C’ is the real component and C” is the imaginary component.

$$C^* = C' - jC'' \qquad \text{(S4)}$$

Since the capacitance of these biosensors may be written as $C = 1/j\omega Z$, C ’and C” are given as a function of electrical impedance by eq. S5 and S6

$$C' = \frac{-Z''}{\omega\left(Z'^2 + Z''^2\right)} \qquad \text{(S5)}$$

$$C'' = \frac{Z'}{\omega\left(Z'^2 + Z''^2\right)} \qquad \text{(S6)}$$

Section 2: Figures

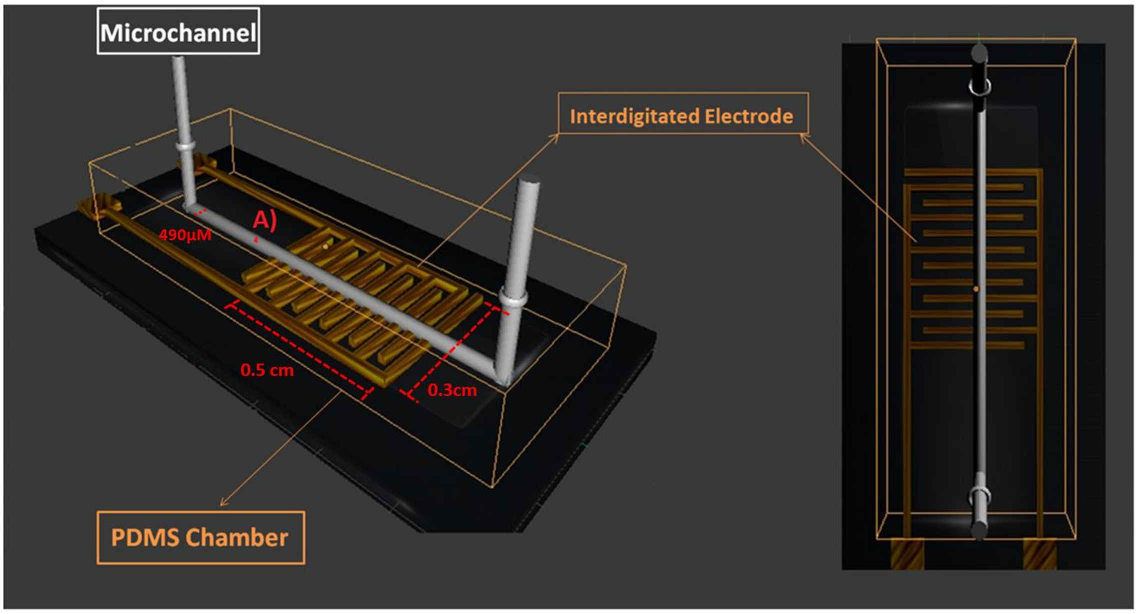

Figure S1: Illustration of the microfluidic chip, formed by gold interdigitated electrode and a PDMS chamber containing the microchannel.

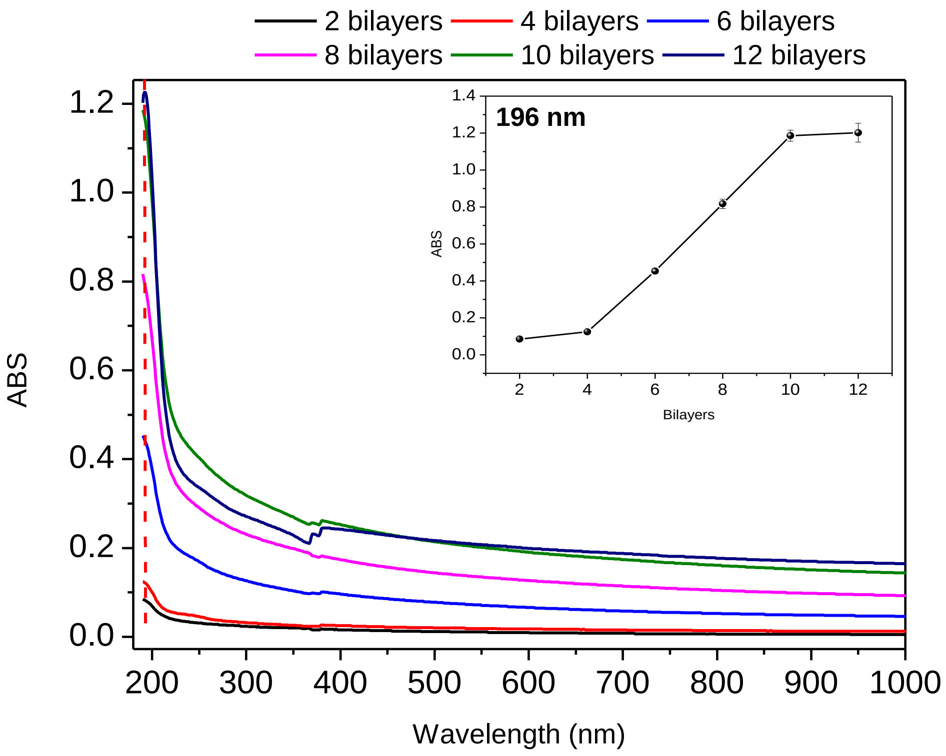

Figure S2: Monitoring of the CHT/CS film bilayers growth by UV-Vis spectroscopy

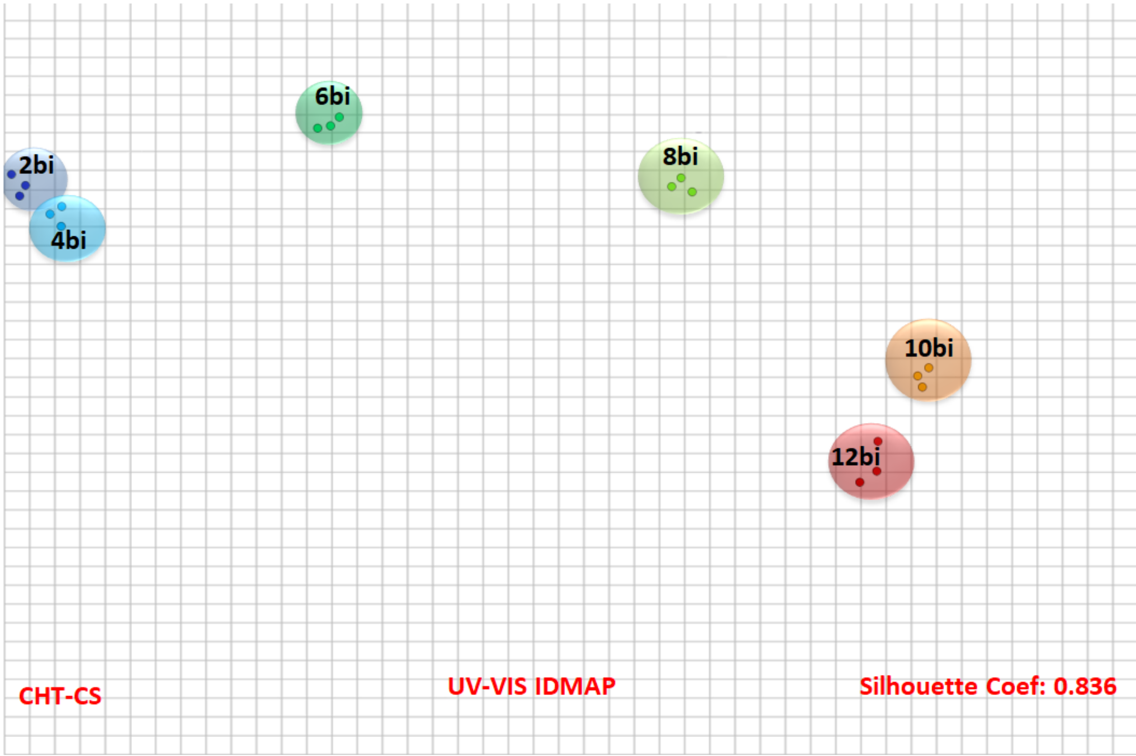

Figure S3: IDMAP Plot for UV-Vis spectra for CHT/CS bilayers. The projections show that the molecular architecture growth stabilizes at 10 bilayers.

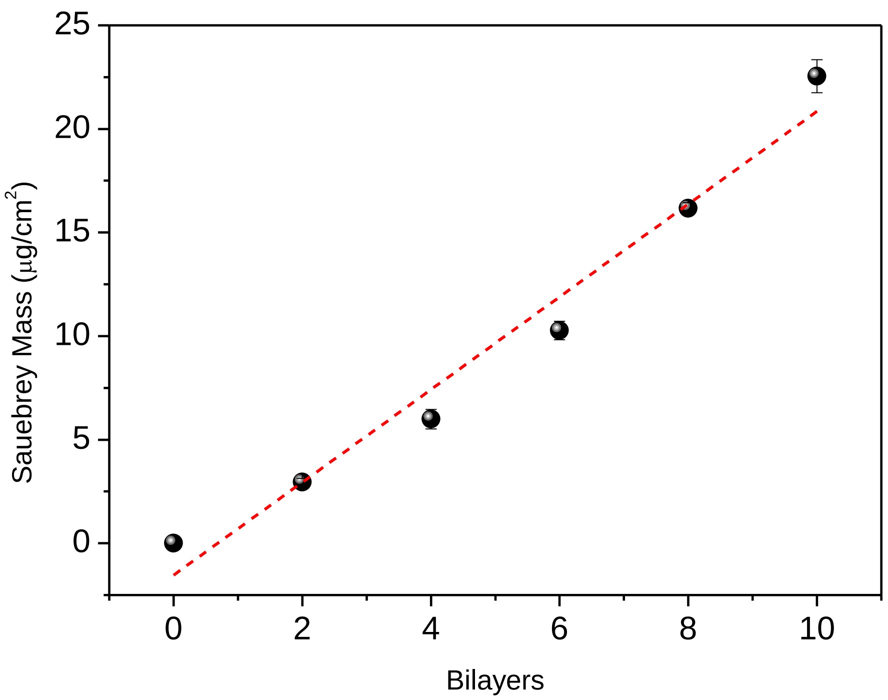

Figure S4: Sauerbrey Mass of each CHT/CS bilayer deposited on the Au electrodes. The bilayers growth was modeled from the linear equation below.

Mass quantification by QCM measurements (Figure S4), modeled by a linear equation (eq. S7-Support Information), where SM is Sauerbrey Mass (μg/cm^2), B is bilayers number.

$$SM = ((2.23 \pm 0.18) \times B) - (1.53 \pm 1.14) \tag{S7}$$

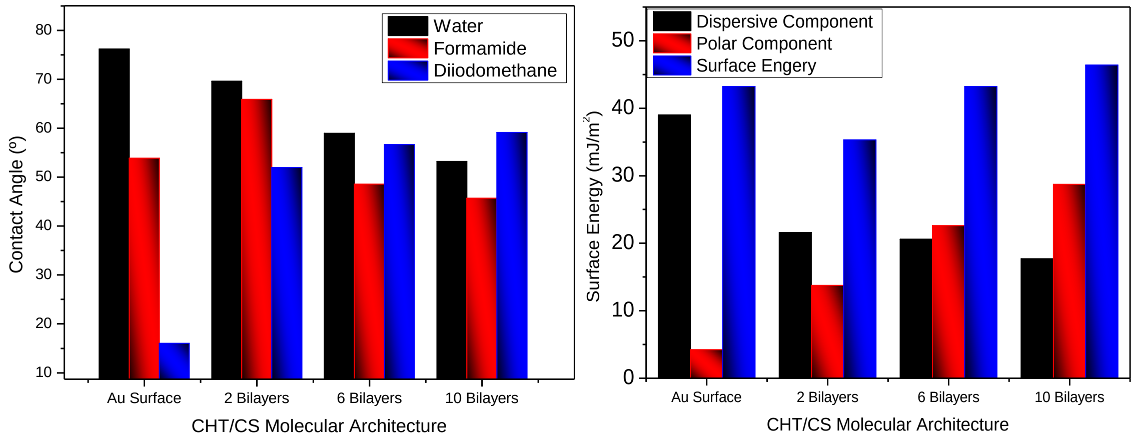

Figure S5: Contact Angle and Surface Energy of CHT/CS molecular architectures with 2, 6 and 10 bilayers.

Section 3: Tables

Table S1: Biosensors available in the literature for detecting mastitis and *S.aureus*. Note that the biosensors developed in this work showed higher sensitivity in relation to the devices found in the literature.

Analytical Method	Limit of Detection (CFu/mL)	Time for Detection	Reference
Potentiometric detection using Electromotive Force (EMF) measured in a SWCNT-aptamer biosensor system	800	---	1
Specific binding of S. aureus in renewable micro-columns using secondary antibodies and fluorescence	200	17 min	2

maker			
Bead Injection Analysis using secondary antibodies and fluorescence markers	100	20 min	3
Point-of-care methodology using magnetic nanoparticles	Above 100	----	4
Fluorescent detection with strand displacement-target recycling amplification	39	----	5
Antibody-hierarchical mesoporous SiO2	11	20 min	6
Au-NP/rGO/glassy carbon sensor	10	60 min	7
Magnetic nanoparticles functionalized with antimicrobial peptides	10	25 min	8
Redox-active gold nanoparticles	10	30 min	9
CHT/CS 6 bilayers (This work)	6.31/6.84	10 min	This work
Electrochemical detection using rGO-Cys electrode	4.4	----	10
CHT/CS 10 bilayers (This work)	2.83/3.93	10 min	This work

Table S2: Assignments of the PM-IRRAS bands responsible for the *S.aureus* detection mechanism.

Wavenumber (1/cm)	**Groups**
1070	• PO_2^- Symmetric Stretching- Phospholipids (S.aureus) • C-O stretch (polypeptides-Antibody)
1229/1232	• C-O-C present in polysaccharides (*S.aureus* cell wall) • N-H, C-N and C-H (aminoacids-Antibody)
1485	CH_2 Bending- Lipids
1547/1550	N-H and C-N groups (Amide II)- Proteins
1648/1651	carbonyl groups (C=O) (Amide I)-Proteins
2860	C-H Sretching Vibration (CH_3)
2940	C-H Sretching Vibration (CH_2)

References

(1) Zelada-Guillén, G. A.; Sebastián-Avila, J. L.; Blondeau, P.; Riu, J.; Rius, F. X. Label-Free Detection of Staphylococcus Aureus in Skin Using Real-Time Potentiometric Biosensors Based on Carbon Nanotubes and Aptamers. *Biosensors and Bioelectronics* **2012**, *31* (1), 226–232. https://doi.org/10.1016/j.bios.2011.10.021.

(2) Peedel, D.; Rinken, T. Rapid Biosensing of Staphylococcus Aureus Bacteria in Milk. *Anal. Methods* **2014**, *6* (8), 2642. https://doi.org/10.1039/c3ay42036a.

(3) Juronen, D.; Kuusk, A.; Kivirand, K.; Rinken, A.; Rinken, T. Immunosensing System for Rapid Multiplex Detection of Mastitis-Causing Pathogens in Milk. *Talanta* **2018**, *178*, 949–954. https://doi.org/10.1016/j.talanta.2017.10.043.

(4) Duarte, C.; Costa, T.; Carneiro, C.; Soares, R.; Jitariu, A.; Cardoso, S.; Piedade, M.; Bexiga, R.; Freitas, P. Semi-Quantitative Method for Streptococci Magnetic Detection in Raw Milk. *Biosensors* **2016**, *6* (2), 19. https://doi.org/10.3390/bios6020019.

(5) Cai, R.; Yin, F.; Zhang, Z.; Tian, Y.; Zhou, N. Functional Chimera Aptamer and Molecular Beacon Based Fluorescent Detection of Staphylococcus Aureus with Strand Displacement-Target Recycling Amplification. *Analytica Chimica Acta* **2019**, *1075*, 128–136. https://doi.org/10.1016/j.aca.2019.05.014.

(6) Wang, H.; Xiu, Y.; Chen, Y.; Sun, L.; Yang, L.; Chen, H.; Niu, X. Electrochemical Immunosensor Based on an Antibody-Hierarchical Mesoporous SiO_2 for the Detection of *Staphylococcus Aureus*. *RSC Adv.* **2019**, *9* (28), 16278–16287. https://doi.org/10.1039/C9RA00907H.

(7) Jia, F.; Duan, N.; Wu, S.; Ma, X.; Xia, Y.; Wang, Z.; Wei, X. Impedimetric Aptasensor for Staphylococcus Aureus Based on Nanocomposite Prepared from Reduced Graphene Oxide and Gold Nanoparticles. *Microchim Acta* **2014**, *181* (9–10), 967–974. https://doi.org/10.1007/s00604-014-1195-8.

(8) Wilson, D.; Materón, E. M.; Ibáñez-Redín, G.; Faria, R. C.; Correa, D. S.; Oliveira, O. N. Electrical Detection of Pathogenic Bacteria in Food Samples Using Information Visualization Methods with a Sensor Based on Magnetic Nanoparticles Functionalized with Antimicrobial Peptides. *Talanta* **2019**, *194*, 611–618. https://doi.org/10.1016/j.talanta.2018.10.089.

(9) Lee, C.-W.; Chang, H.-Y.; Wu, J.-K.; Tseng, F.-G. Ultra-Sensitive Electrochemical Detection of Bacteremia Enabled by Redox-Active Gold Nanoparticles (RaGNPs) in a Nano-Sieving Microfluidic System (NS-MFS). *Biosensors and Bioelectronics* **2019**, *133*, 215–222. https://doi.org/10.1016/j.bios.2019.03.040.

(10) Wu, Y.; Chai, H. Development of an Electrochemical Biosensor for Rapid Detection of Foodborne Pathogenic Bacteria. *Int. J. Electrochem. Sci.* **2017**, 4291–4300. https://doi.org/10.20964/2017.05.09.